Long-Term Fluctuations of Water Temperatures in the Upper 200*m* off the Southeast Coast of Korea*

Yong-Q. KANG and Hye-Eun KANG
Department of Oceanography, National Fisheries University of Pusan, Pusan 608-737, Korea

The thermal structures and their spatio-temporal fluctuations in the upper 200*m* layer off the southeast coast of Korea are studied using the bimonthly temperature data for 17 years(1967~1983) at 37 stations. We analyzed the fluctuations of the temperatures in the surface(0~100*m*) and in the subsurface(100~200*m*) layers. The fluctuations of temperatures in the surface water are dominated by the annual variation, whereas the subsurface layer temperatures contain considerable non-seasonal fluctuations. The distributions of water temperature anomalies in the subsurface layer are closely related with those in the surface layer. The predominant periods of temperature fluctuations in the subsurface layer, other than the annual variation, are 14 and 70 months. The period of 14 months coincides with that of the pole tide or Chandler wobble. The cluster analysis shows that our study area can be divided into the cold, the frontal and the warm regions.

Introduction

The spatio-temporal variabilities of the sea water temperasture in the southwestern part of the East Sea of Korea(Japan Sea) are closely related with the ocean current system in that region. The currents in our study area(Fig. 1) consist of the East Korea Warm Current flowing northward and the North Korea Cold Current flowing southward along the east coast of Korea. The extensions of the East Korea Warm Current and of the North-Korea Cold Current, after they leave the coast, form the Polar Thermal Front in the East Sea of Korea. The Polar Thermal Front has a meandering feature near the Ullung Island.

In our previous paper(Kang and Kang, 1990) we limited our study to the descriptions of spatio-temporal characteristics of the 'Ullung Warm Lens'. In this paper we extend our study to the spatio-temporal variabilities of water temperatures in the upper 200*m* layer off the southeast coast of Korea.

The fluctuations of water temperatures in the

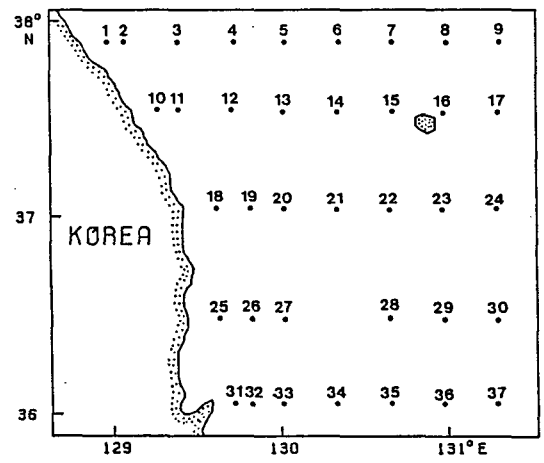

Fig. 1. Oceanographic stations of the National Fisheries Research and Development Agency in our study area.

This study was supported by the Korea Science and Engineering Foundation, 1988, and by the Basic Science Research Institute Program, Ministry of Education, 1989.
Contribution No. 275 of Institute of Marine Sciences, National Fisheries University of Pusan.

upper 100*m* layer are dominated by seasonal variation, whereas those in the subsurface layer are controlled mainly by advections of heat associated with ocean currents. In this paper we considered the water temperatures in the surface layer(0~100 *m*) and those in the subsurface layer(100~200*m*) separately.

The spatio-temporal distributions of the water temperatures in both layers are analyzed by the statistical, the empirical orthogonal function, the spectral and the cluster analyses. We have paid a special attention to the temporal and spatial correlations between the anomalies in the surface and subsurface layers.

The Data

The data used in this study are the bimonthly serial obsrvations of water temperatures by the National Fisheries Research and Development Agency(NFRDA) of Korea for 17 years(1967~1983) at 37 stations shown in Fig. 1. The standard depths of observation within the upper 200*m* are 0, 10, 20, 30, 50, 75, 100, 125, 150 and 200*m*. The bimonthly normals of water temperature at each station and depth are computed from the observed data during the 17 years. The data coverage is 91%, and the remaining 9% of the missing data are interpolated by linear interpolations of the temperature anomalies.

The vertically averaged water temperature $T_1(x, y, t)$ in the surface layer(0~100*m*) and that $T_2(x, y, t)$ in the subsurface layer(100~200*m*) are defined by

$$T_1(x, y, t) = \frac{1}{100}\int_{0m}^{100m} T(x, y, z, t)\, dz$$

$$T_2(x, y, t) = \frac{1}{100}\int_{100m}^{200m} T(x, y, z, t)\, dz$$

where $T(x, y, z, t)$ is the water temperature at location(x, y), depth z and time t. The vertically averaged temperatures, T_1 and T_2, are computed from the water temperatures at the standard depths by using the trapezoidal rule. The bimonthly time series of vertically averaged temperatures in the surface and those in the subsurface layers for 17 years at 37 stations are used as the basic data set for our study.

Fluctuations of Water Temperatures

The overall features of the thermal variability in our study area are represented by the distributions of the mean and the root-mean-square(RMS) amplitudes of the temperature fluctuations in the surface and in the subsurface layers. The temporal changes of water temperatures are represented by the time series of average temperatures, that is, the average over 37 stations in each layer.

The Surface Layer

Fig. 2 shows the distributions of the means and the RMS amplitudes of temperature fluctuations, and also the time series of the average temperatures in the surface layer(0~100*m*). The mean temperatures in the surface layer are between 8 and 14℃. The isotherms of the mean temperatures in the coastal region within 100*km* from the coast area almost parallel to the coastline(Fig. 2(a)). The mean temperatures near the coast are lower than those in offshore at the same latitudes. The RMS amplitudes of temperature fluctuations in the surface layer are between 2.8 and 3.8℃(Fig. 2(b)).

The time series of average water temperatures (Fig. 2(c)) shows that the temperature fluctuations in the surface layer down to 100*m* are dominated by annual variation. However, the annual march of the temperature differs significantly from year to year. For example, the surface water temperatures in 1974 and 1981 were much lower than those in other years.

Subsurface Layer

Fig. 3 shows the distributions of the means and the RMS amplitudes and also the time series of the average temperatures in the subsurface layer of 100~200*m*. The isotherms of the mean temperature in the subsurface layer within 100*km* from the coast are almost parallel to the coast(Fig. 3(a)). The RMS amplitudes of the subsurface temperature fluctuations near the coast are smaller than those in offshore region(Fig. 3(b)). In particular,

the fluctuations of subsurface water temperature in the region just south of Ullung Island, where the phenomena of so called 'Ullung Warm Lens' occurs(Kang and Kang, 1990), are relatively smaller than those in the bordering region. The time series of the average temperatures(Fig. 3(c)) shows that the non-annual fluctuations play a significant role in the variations of subsurface water temperatures.

Vertical Correlation of the Anomalies

Although the distributions of the sea surface temperatures(SST) can be monitored by the satellite remote sensing, there remains a question whether the temperatures in the subsurface layer can be inferred from the distribution of the SST or not. With that question in mind, we computed the similarity between the anomalies of water temperatures in the surface layer and in the subsurface layer by two approaches. First, we computed the correlations between the time series of the horizontally averged temperatures in the surface layer and in

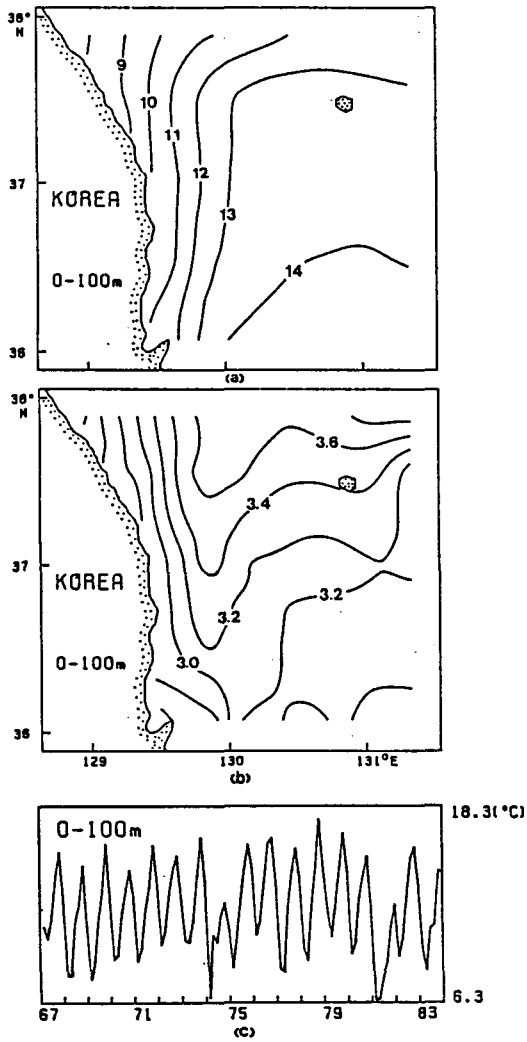

Fig. 2. Water temperatures in the surface layer(0~100m). (a)The means, (b)the standard deviations, and (c)the time series of the average temperatures.

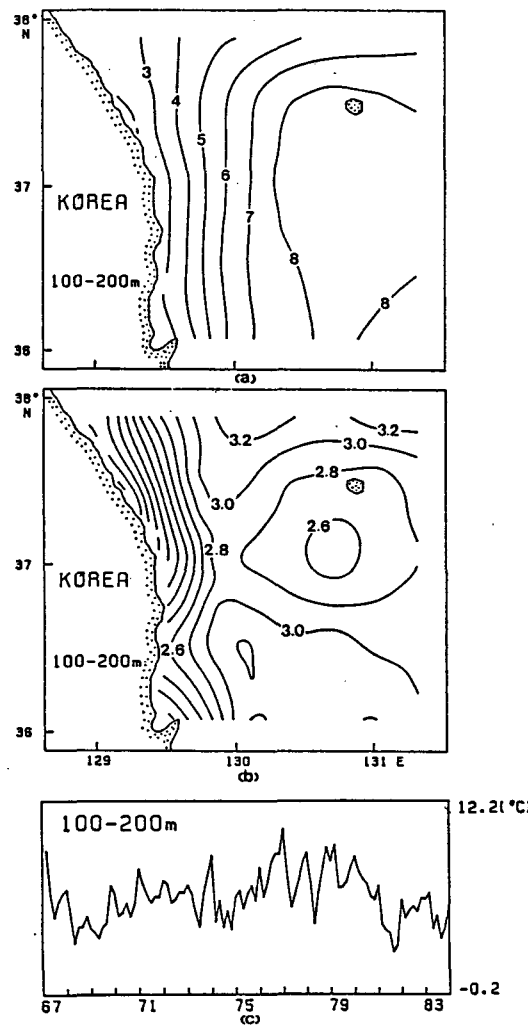

Fig. 3. Water temperatures in the subsurface layer (100~200m). (a)The means, (b)the standard deviations, and (c)the time series of the average temperatures.

the subsurface layer. Secondly, by employing the spatial correlation, we estimated the similarity between distribution patterns of temperature anomalies in the surface and subsurface layers at the same time.

Temporal Correlation

Fig. 4(a) shows the time series of the horizontally averaged water temperature anomalies in the surface(0~100*m*) and in the subsurface layer (100~200*m*). The correlation coefficients between the two time series is 0.785. This figure shows that the temperature anomalies in two layers are highly correlated. It implies that the average temperature anomaly in the subsurface layer can be inferred by using the average temperature anomaly in the surface layer.

Spatial Correlation

Although the time series of the average temperature anomalies are highly correlated, there remains a question whether the regional distributions of the temperature anomalies in two layers are similar or not. To answer that question, we estimated the similarity in the distributions of anomalies in two layers at time t by the 'map correlation' $C(t)$ defined by

$$C(t)=\frac{\sum_{i=1}^{m} T_1(j,t)\ T_2(j,t)}{[\sum_{i=1}^{m} T_1^2(j,t)\ \sum_{i=1}^{m} T_2^2(j,t)]^{1/2}}$$

where $T_1(j,t)$ and $T_2(j,t)$ are temperature anomalies at time t at j^{th} station in the surface and subsurface layers, respectively, and m is the number of stations($m=37$). The spatial correlation $C(t)$ defined by above equation is similar to the definition of the correlation coefficient, except that the overall mean is not removed in computing the spatial correlation. If distribution patterns of anomalies in two layers at time t are completely similar, then $C(t)$ becomes to 1. If two distribution patterns are 'mirror images' of each other, then $C(t)$ becomes to -1.

Fig. 4(b) shows the map correlations between the anomaly patterns in the surface and in the subsurface layers. The map correlations in our study area during the past 17 years(1967~1983) varied between 0.25 and 0.91, and their average value was 0.656. Although the values of map correlation differ from month to month, there were no cases with negative map correlations.

The rather large values of temporal correlation coefficient between the time series of the average temperature anomalies and the map correlations between the distribution patterns of anomalies in two layers indicate that the temperature anomalies in the subsurface layer(100~200*m*) are closely related with those in the surface layer(0~100*m*).

EOF Analysis of the Subsurface Temperatures

Method of EOF Analysis

The spatio-temporal distribution of time series at many stations can be represented by the empirical orthogonal functon(EOF) or eigenfunction alaysis.

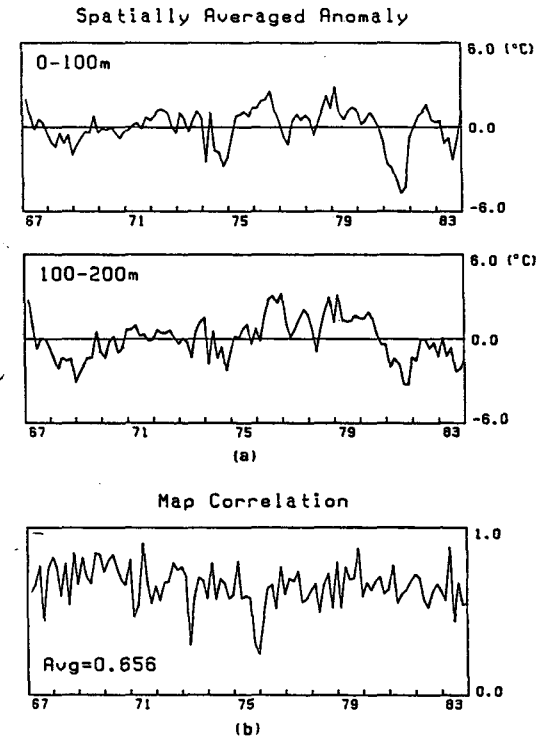

Fig. 4. (a)The anomalies of the average temperature in the surface layer(0~100*m*) and in the subsurface layer(100~200*m*) in 1967~1983. (b)The map correlations between the distribution patterns of temperature anomalies in the surface and the subsurface layers.

In the EOF analysis, a set of time series, $T(x, t)$, of each length n at m locations is represented by a superposition of m modes by

$$T(x, t)=\sum_{i=1}^{m} e_i(x)\ c_i(t),$$

where $e_i(x)$ is the eigenvector or eigenfunction that describes the spatial distribution of temperature associated with the *i-th* mode, and $c_i(t)$ is the time-dependent coefficient that describes the temporal characteristics associated with the *i-th* mode. The eigenvectors and the time-dependent coefficients associated with different modes are required to be orthogonal. That is,

$$\sum_{x=1}^{m} e_i(x)\ e_j(x)=\delta_{ij},$$

$$\sum_{t=1}^{n} c_i(t)\ c_j(t)=n\,\delta_{ij}.$$

The normalized eigenvector e is found by solving an eigenvalue problem

$$Re=\lambda e,$$

where R is the m by m covariance matrix of the time series at m locations, and λ is the eigenvalue. The time-dependent coefficients $c_i(t)$ are proportional to the fluctuations of temperature. However, due to the orthonormality condition, the magnitudes of the time-dependent coefficient are not the same as the physical magnitude. More details of the EOF method can be found in Kutzbach(1967).

Results of EOF Analysis

The spatio-temporal characteristics of bimonthly water temperatures in the subsurface layer for 17 years at 37 stations are represented by the EOF analysis. The results of the EOF analysis of the subsurface water temperatures are as follows. More than half of the total variance are explained by superposition of 3 EOF modes. The percentages of variance explained by the first 3 modes are 36, 10 and 9%, repsectively. Figs. 5, 6 and 7 show the eigenvectors, the time series of the time-dependent coefficient and the power spectra of the time series associated with the first 3 EOF modes, respectively. The power spectrum is computed by the Fourier transform of the autocovariance function(Jenkins and Watts, 1968).

The results of the first EOF mode, which covers 36% of variance, are shown in Fig. 5. The identical sign of the eigenvectors at all stations(Fig. 5(a)) implies that the subsurface temperatures associated with the first mode fluctuate simultaneously. The time series of the time-dependent coefficient of this mode(Fig. 5(b)) is remarkably similar to that of

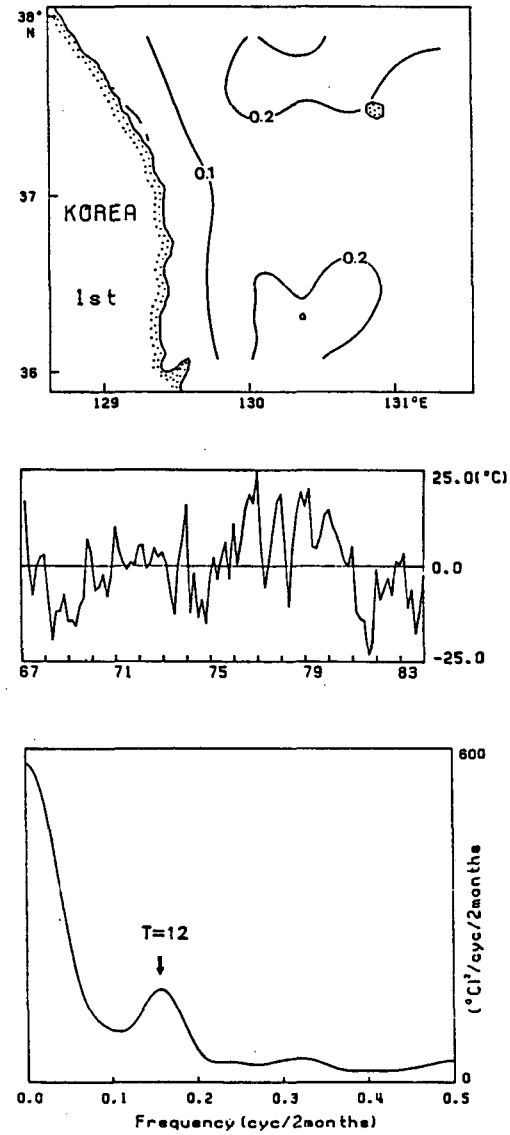

Fig. 5. The first EOF mode of the fluctuations of the subsurface water temperatures in 1967~1983. (a)The eigenvector, (b)the time series of the time-dependent coefficients, and (c)the power spectrum of the time series. The first mode, which explains 36% of the variances, is dominated by the annual variations.

the average subsurface temperature fluctuations (Fig. 3(c)). The power spectrum of the time-dependent coefficient shows that temporal change of this first mode is characterized by the annual variation and long-term variation.

The results of the second EOF mode, which covers 10% of the variance, are shown in Fig. 6. The distribution of the eigenvectors is characterized by the positive values in the southeastern part and the negative values in the northwestern part(Fig. 6(a)). That is, the signs of eigenvectors of the second mode in the East Korea Warm Current region are opposite to those in the north Korea Cold Current region. The time series of the time-dependent coefficients associated with the second mode is shown in Fig. 6(b). Power spectrum of the time series shows that the most predominant period associated with this mode is 14 months(Fig. 6(c)). Note that this period of 14 months coincides with the period of pole tide or Chandler Wobble.

The results of the third EOF mode, which covers 9% of the variance, are shown in Fig. 7. According to the distribution of positive eigenvectors in the southern part and negative eigenvectors in the northern part, this mode is characterized by off-phase fluctuations between northern and southern parts(Fig. 7(a)). The spectrum(Fig. 7(c)) of the time series(Fig. 7(b)) shows that the most predominant period associated with this mode is 70 months.

Cluster Analysis

As mentioned earlier, waters in our study area are carried by the North Korea Cold Current from the north and the East Korea Warm Current from the south. In order to identify the subareas with similar thermal characteristics, we made cluster analysis on the 'average' differences of subsurface water temperature among 37 stations in our study area. The average difference is defined as the arithmetic mean of the differences over 17×6 bi-monthly data during the 17 years. Details on the cluster analysis can be found, for example, in Murtagh and Heck(1987).

Fig. 8(a) shows the dendrogram of the clusters based on the similarity of average differences of subsurface temperatures among 37 stations in 17 years(1967~1983). The dendrogram in Fig. 8(a) suggests that our study area can be grouped into 3 subareas. Fig. 8(b) shows the subdivisions of our

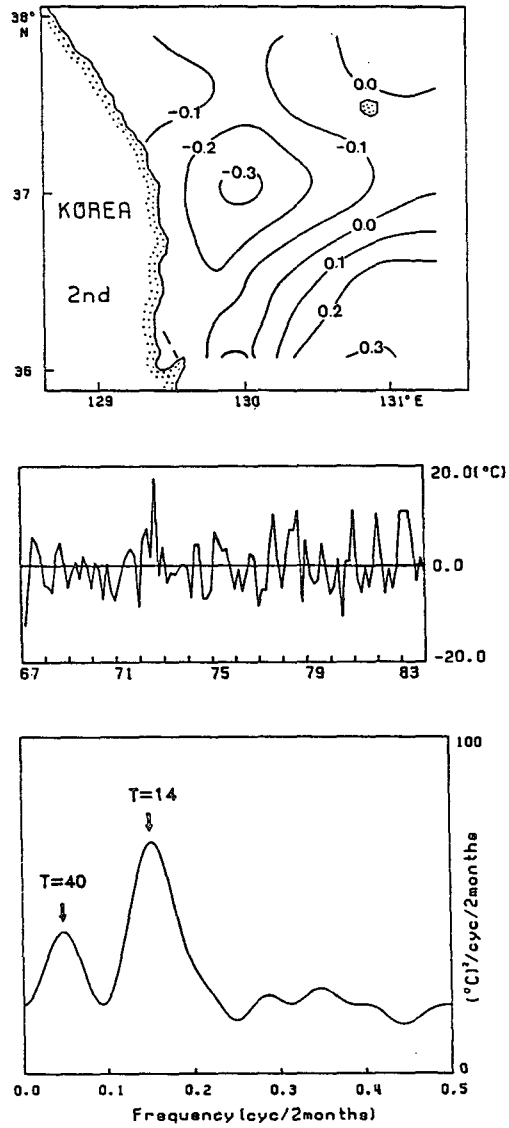

Fig. 6. The second EOF mode of the fluctuations of the subsurface water temperatures. This mode, which explains 10% of the variance, is dominated by the fluctuations with a period of 14 months.

study area. As shown in Fig. 8(b), our study area can be subdivided into (A) the cold water region, (B) the frontal or transitional region, and (C) the warm water region.

Discussion and Conclusions

The distributions and fluctuations of seawater temperatures in the surface(0~100*m*) and subsurface(100~200*m*) layers off the southeast coast of Korea are presented in this paper. The isotherms within 100*km* from the coast in both layers are almost parallel to the coastline. This implies that the ocean currents near the coast flow almost parallel to the coast.

The fluctuations of water temperatures in the surface layer are dominated by annual variation. The annual variations of temperature generally de-

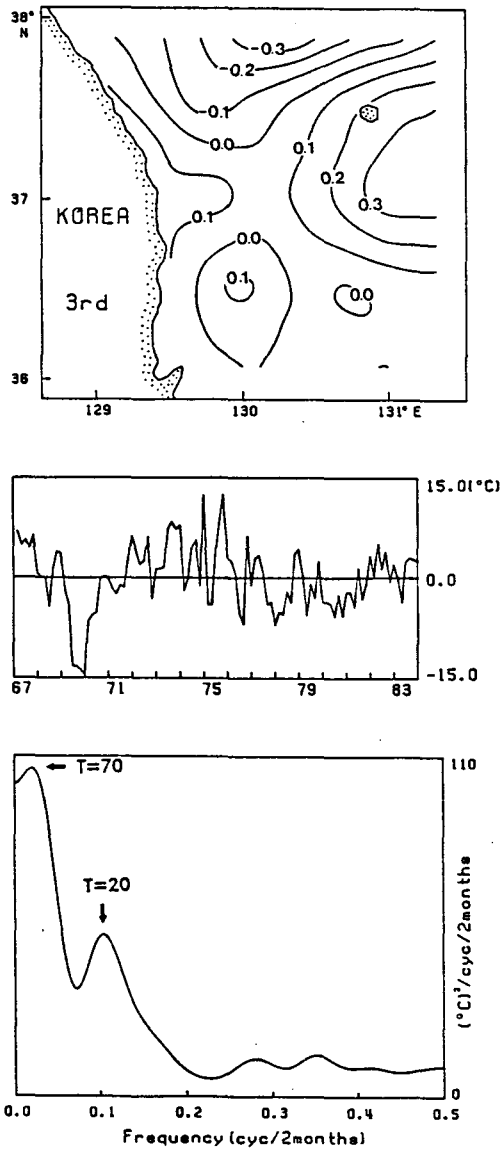

Fig. 7. The third EOF mode of the fluctuations of the subsurface water temperatures. This mode, which explains 9% of the variance, is dominated by the fluctuations with a period of 70 months.

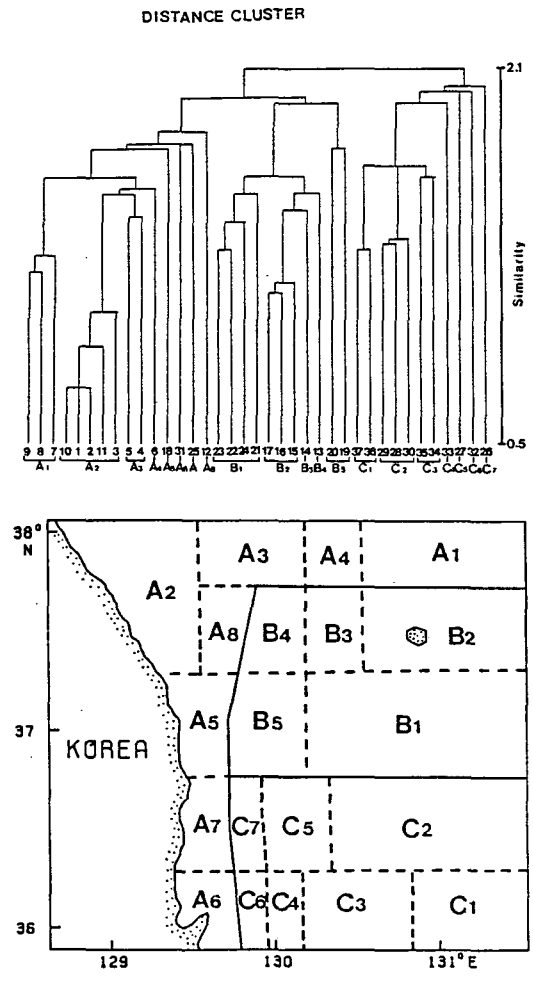

Fig. 8. Results of the cluster analysis of the subsurface water temperatures in 1967~1983. (a) The dendrogram based on the temperature differences among 37 stations, and (b) the subareas of our study area based on the similarities of the temperature differences.

crease with depths. In the subsurface layer of 100~200*m*, non-annual fluctuations become important. The predominant periods of temperature fluctuations in the subsurface layer associated with the time series of the first 3 EOF modes are 12, 14 and 70 months, respectively. The time series of the fourth EOF mode is dominated by 33 months fluctuations (the results of fourth mode is not presented).

The 14 months fluctuations, which is the most dominant period in the time series of the second EOF mode of subsruface temperature, coincide with the period of the pole tide or Chandler wobble. The pole tide with periods of 14 months are reported to occur in the monthly sea levels(Sarukhanyan, 1969; Lisitzin, 1974; Thomson, 1980) and also in the fluctuations of ocean currents(Maximov, *et al.*, 1972). The 14 months fluctuations are also reported to occur in the geophysical time series inside or near Korean Peninsula. The SST anomalies off the southeast coast of Korea(Gong and Kang, 1986) and those at coastal stations along the Tsushima Current region(Kang and Choi, 1985) show 14 months fluctuations. Also the air temperature anomalies at all of 14 standard meteorological stations in Korea also show fluctuations with the pole tide period(Kang and Rho, 1985).

The predominant period associated with the 3rd EOF mode is 70 months. It is interesting to note that the air temperature anomalies in Korea also show predominant fluctuations with a similar period. Kang and Rho(1985) reported that the air temperature anomalies at 12 stations among 14 stations in Korea showed spectral peaks at 72 months.

In this paper we showed that the water temperature anomalies in the subsurface layer(100~200*m*) are highly correlated with those in the surface layer(0~100*m*). The temporal correlation between the average time series of anomalies in two layers is 0.785. The map correlations between the distribution patterns of anomalies in two layers are always positive, and their average value is 0.656. This feature suggests that the distributions of the temperature in the subsurface layer up to 200*m* can be inferred to a certain degree from the distributions of the SST, which can be monitored by the satellite remote sensing technique.

References

Gong, Y. and Y. Q. Kang. 1986. Sea surface temperature anomalies off the southeastern coast of Korea. *Bull. Fish. Res. Dev. Agency,* **37**, 1~9.

Jenkins, G. M. and D. G. Watts. 1968. *Spectral Analysis and Its Applications.* Holden-Day, 525pp.

Kang, Y. Q. and S. -W. Choi. 1985. Annual and interannual fluctuations of coastal water temperatures in the Tsushima Current and the Kuroshio regons. *Bull. Kor. Fish. Soc.,* **18**(6), 497~505.

Kang, H. -E. and Y. Q. Kang. 1990. Spatio-temporal characteristics of the Ullung Warm Lens. *Bull. Kor. Fish. Soc.,* **23**(5), 407~415.

Kang, Y. Q. and C. -S. Rho. 1985. Annual and interannual fluctuations of air temperature in Korea during the past 30 years(1954~1983). *J. Kor. Meteor. Soc.,* **21**(3), 1~10.

Kutzbach, J. E. 1967. Empirical eigenvectors of sea-level pressure, surface temperature and precipitation complexes over North America. *J. Appl. Meteor.,* **6**, 791~802.

Lisitzin, E. 1974. *Sea Level Changes,* Elsevier Publ., 286pp.

Maximov, I. V., E. I. Sarukhanyan and N. P. Smirnov. 1972. Long-term variations of the North Atlantic Current and their possible causes. *Rapp. Proc. -Verb. Reun., Cons. Int. Explor. Mer,* **162**, 159~166.

Murtagh, F. and A. Heck. 1987. *Multivariate Data Analysis.* D. Reidel Publ., 210pp.

Sarukhanyan, E. I. 1969. Polar tide in the ocean. *Dokl. Akad. Nauk SSSR,* **188**, 571~574(English Trans., *Geophysics,* **188**, 7~10).

Thomson, K. R. 1980. An analysis of British monthly mean sea level. *Geophys. J. Roy. Astro. Soc.,* **63**, 57~73.

Received October 11, 1991
Accepted November 9, 1991

한국 동해안 외해 표층 200*m* 수온의 장기변동

강용균 · 강혜은
부산수산대학교 해양학과

국립수산진흥원의 격월별 17년간(1967~1983) 37개 정점의 해양조사 자료를 이용하여 한국 동해안 외해 표층 200*m* 해수의 열적 구조와 수온의 시공간적 변동을 구명하였다. 표층(0~200*m*)과 아표층(100~200*m*)의 수온 변동을 분석하여 도출된 주요 결과는 다음과 같다. 표층에서의 수온 변동은 주로 1년 주기의 계절적 변동이 대부분이지만, 아표층의 수온 변동에서는 비계절적인 변동이 우세하다. 하지만, 계절적인 예년변동치를 제거한 수온 이상변동의 경우, 표층과 아표층의 수온 이상변동은 시간적으로 밀접한 상관관계가 있을 뿐만 아니라 공간적인 분포도 유사성이 크다. 아표층의 수온 변동은 1년 주기 이외에 14개월과 70개월의 탁월주기를 가진다. 아표층에서 나타나는 14개월 주기의 수온 변동은 극조(pole tide, Chandler wobble)의 주기와 일치한다. 아표층 해역 수온 변동에 대한 군집해석에 의하면, 이 해역은 한류역, 천이역 및 난류역으로 구분된다.